International Journal of Engineering and Advanced Technology (IJEAT)
ISSN: 2249-8958 (Online), Volume-9 Issue-2, December, 2019

Sol-Gel Synthesized N and MN Co-Doped Tio_2 Nanomaterial for Photocatalytic Degradation of Malathion under Visible Light Irradiation

Susmitha Thota, Gollamudi Padma Rao, Imandi Manga Raju, Siva Rao Tirukkovalluri

Abstract: ***Different weight percentages (0.25-1.00 wt%) of Nitrogen (Non-Metal) and Manganese (Metal) co-doped nano titania were synthesized by sol-gel method and characterized by XRD, UV-vis.DRS, FT-IR, XPS, SEM and TEM. The XRD results has shown that all the prepared catalysts are in anatase phase indicating that co-doping of N and Mn did not affect the crystal structure of TiO_2. From the UV-vis.DRS spectra a significant absorption shift towards visible region was noticed in N and Mn co-doped TiO_2 and their presence was confirmed by XPS and FT-IR results. SEM and TEM results showed spherical nanoparticles with average particle size of 9 nm. Photocatalytic efficiency of synthesized nano materials was tested on non-biodegradable organophosphorous pesticide, Malathion under visible light irradiation. The effect of dopant concentration, pH, catalyst dosage, and initial pesticide concentration on photocatalytic degradation of malathion was studied and optimum conditions were established. Among the synthesized samples 0.50 wt% N & 1.00 wt% Mn-TiO_2 exhibited best photocatalytic performance. Photoluminiscent spectroscopy (PL) was used to examine the rate of production of oxidative species, hydroxyl radicals which play key role in photocatalytic degradation.***

Keyword**: Malathion, Manganese, Nitrogen, Sol-gel method, Titanium dioxide, Visible light.**

I. INTRODUCTION

Environmental problems, attentively agricultural waste waters containing pesticides concerned as a serious problem in developing countries [1]. In particular, agriculture drain water contains large quantities of Malathion due to its extensive use in various agricultural applications [2]. Malathion(S-1,2-bis(ethoxicarbonyl)ethyl 0,0-dimethyl-phosphorodithioate) is a relatively water soluble organophosphorous pesticide, which is highly toxic toward aquatic organism, amphibian, vertebrate, and even human beings [3]. Therefore, it is necessary to investigate new methods for decontamination of malathion from agriculture waste water. Heterogeneous photocatalysis has been experimentally shown to be a promising method and an emerging technique for degrading a wide range of pesticides in water due to its simplicity, reusability and low cost [4, 5]. Because of its advantages like long term stability, inexpensive, non-toxicity and good adsorption efficiency, anatase titanium dioxide has universally recognized as one of the best heterogeneous photocatalysts [6, 7]. Although TiO_2 is superior over other photocatalysts for wide practical applications its wide energy band (3.2 eV) and high recombination rate of electron-hole limits its visible light activity leads to low quantum efficiency [8]. Therefore, recent research attention is focused on the modification of TiO_2 sensitive to visible light by metal and non-metal ion doping, dye or polymer sensitization and semiconductor coupling [9-12]. Among the above, co-doping of TiO_2 with metal and a non-metal proves beneficial [13, 14]. According to previous reports, the non-metal dopant can shift the absorbance region of TiO_2 from ultraviolet to visible part of the spectrum. In addition to narrowing the band gap of TiO_2 the metal dopant can decrease the rate of electron-hole recombination [7, 15]. It is important to fabricate a photocatalyst with suitable crystal phase, particle size and surface morphological properties to enhance its photocatalytic activity. Hence, in this work we have selected Manganese (Mn) and Nitrogen (N) as metal and non-metal dopants to be co-doped into TiO_2 and study its catalytic activity under visible light irradiation. Among the different methods like hydrothermal, solvothermal [16], chemical vapour deposition [17], precipitation [18], and electro spinning [19], sol-gel method is preferable for the synthesis of TiO_2 photocatalyst, because at very low temperatures and under stoichiometry control the catalysts of homogenous concentrations with high purity can be synthesized [20]. Hence, for the synthesis of Nitrogen and Manganese co-doped TiO_2 photocatalysts sol-gel synthesis process has been followed.

II. MATERIALS AND METHODOLOGY

A. Materials used

Titanium tetra-n-butoxide (Ti (O-Bu)$_4$), Manganese nitrate ($Mn(NO_3)_2$) and Urea (CH_4N_2O) procured from E. Merk (India) were used as precursors of Ti, Mn and N for the synthesis of co-doped TiO_2. Milli Q water, ethanol and nitric acid were used for solutions preparation. Malathion is used as a model pesticide pollutant for photodegradation application.

Revised Manuscript Received on December 30, 2019.

* Correspondence Author

Sushmitha Thota, Department of Inorganic & Analytical Chemistry, School of Chemistry, Andhra University Visakhapatnam, India. Email: susi.thota@gmail.com

Gollamudi Padma Rao, Department of Chemistry, Dr. B.R. Ambedkar Univsity, Srikakulam, Andhrapradesh, India. Email: pgollamudi777@gmail.com

Imandi Manga Raju, Department of Inorganic & Analytical Chemistry, School of Chemistry, Andhra University Visakhapatnam, India. Email: mangorchem@gmail.com

Tirukkovalluri Siva Rao, Department of Inorganic & Analytical Chemistry, School of Chemistry, Andhra University Visakhapatnam, India. Email: sivaraoau@gmail.com

All the mentioned chemicals are of analytical grade and used as received without further purification.

B. Synthesis of photocatalysts

A series of TiO_2 samples were synthesized by co-doping of N and Mn in low-concentration range (0.25-1.00 wt%) along with undoped TiO_2 using sol-gel method, because high level doping will create many lattice defects, which can acts as electron-hole recombination centres [21, 22]. In this method, desired wt% of N and Mn from their precursors were first dissolved in ethanol and added water. Under vigorous stirring the resultant solution was added drop wise to another solution of $Ti(OBu)_4$ dissolved in ethanol and acidified with nitric acid. The colloidal suspension obtained was stirred for 90 min and aged for 48 h. The gel obtained was dried in an oven at 70 ºC, ground and calcined at 400 ºC for about 5 h. Finally, the homogeneous powder is obtained after well ground using mortar pestle. The undoped TiO_2 was synthesized in the same process without adding dopant precursors. Details of all the co-doped samples are given in table 1.

Table.1. Different N and Mn co-doped TiO_2 nanocatalysts.

S.No	Name of the catalyst	Name assigned to catalyst
1	0.25 Wt% N-1.00 Wt% Mn	NMn1
2	0.25 Wt% N-0.75 Wt% Mn	NMn2
3	0.50 Wt% N-0.50 Wt% Mn	NMn3
4	0.75 Wt% N-0.25 Wt% Mn	NMn4
5	1.00 Wt% N-0.25 Wt% Mn	NMn5
6	1.00 Wt% N-0.50 Wt% Mn	NMn6
7	0.50 Wt% N-1.00 Wt% Mn	NMn7
8	Undoped TiO_2	

C. Experimental Techniques used for the characterization of photocatalysts

X-ray Diffraction (XRD) analysis was done by X-Ray diffractometer (model Ultima IV, RIGAKU) using Anod CuKα (λ=1.541A°) radiation with a nickel filter for 2θ from 20° to 80°. Shimadzu 3600 UV-visible NIR Spectrophotometer with an integrating sphere diffuse reflectance accessory was used to obtain the Diffuse reflectance spectra (DRS) using $BaSO_4$ as reference scatter. FT-IR spectrometer (Nicolot Avatar 360) was used to record the FT-IR spectra of the samples. PHI quantum ESCA microprobe system using AlKα radiation of 250W X-ray tube as a radiation source with energy of 1486.6 eV, 16 mA × 12.5 kV was used to record X-Ray photoelectron spectra (XPS) under working pressure lower than 1×10^{-8} Nm^{-2}. The Surface morphology and particle size were characterized by scanning electron microscope (SEM) (JSM-6610LV) operated at 20 kV and transmission electron microscope (TEM) (TECNAI FE12) operated at 120 kV. Degradation patterns of malathion was analyzed using UV-vis spectrophotometer (Shimadzu 1601). Hitchi F-7000 fluorescence spectrophotometer was used for the Photoluminescence (PL) measurements of the samples.

D. Photocatalytic activity study of catalyst

Malathion solution containing the catalyst was stirred in dark for 20 min to attain the adsorption-desorption equilibrium on the catalyst surface. Then the solution was exposed to visible light produced from 400W high pressure mercury vapour lamp (Osram, India). At certain regular time intervals, 5 mL samples were collected through 0.45µm Millipore syringe filter. The filtrate was analyzed on spectrophotometer from 200-800 nm. Malathion has a characteristic absorption band at 266 nm [23] and another peak was also observed at 214 nm. However, the rate of degradation was examined by the decay of these bands using UV-vis spectroscopy. The degradation percentage of malathion was calculated from below equation:

$$\% \text{ of Degradation} = A_o\text{-}A_t / A_o \times 100$$

Where, A_o and A_t are initial and final absorbance of malathion solution before and after the degradation time (t), respectively.

III. RESULT AND DISCUSSION

A. XRD and TEM Analysis:

The phase structure of co-doped and undoped TiO_2 samples after calcinations was determined by XRD patterns and represented in Fig. 1. The XRD patterns observed at 2θ=25.3º of high intensity is attributed to (101) plane of anatase TiO_2 (JCPDS File no: 21-1272). In addition, 37.7º, 47.9º, 54.1º patterns of intensity represents the (004) (200) (211) crystal planes of anatase TiO_2. From XRD patterns it is confirmed that co-doping has no affect on the TiO_2 crystal patterns and transition of anatase crystal phase was resulted due to calcinations at 400 ºC. There are no characteristic peaks of Mn and N oxides were observed, which indicates that the Mn and N are incarporated into lattice of anatase TiO_2. By applying Scherrer formulae to the strongest peak (101) the crystallite size of all synthesized catalysts were calculated and found to be ranging from 9.9 to 11.6 nm.

It was noticed that upon Mn dopant concentration increase, the size of anatase crystallite is slightly decreasing from 12.5 nm for undoped TiO_2 down to 9.9 nm for TiO_2 doped with 1.00 wt% Mn. This is may be attributed to increasing metal doping concentration can suppresses the crystal growth [24].

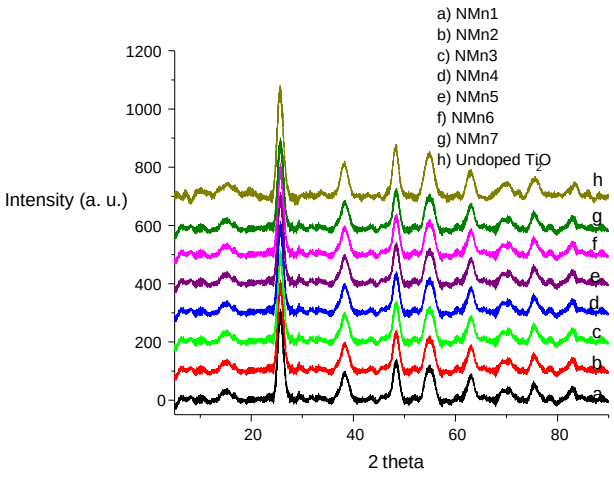

Fig.1 XRD patterns of undoped and N & Mn co-doped TiO_2 catalysts.

B. UV-vis DRS Studies

The UV-vis.DRS spectra of synthesized catalysts are depicted in Fig. 2. It was noticeably found that the absorption band edge of anatase TiO_2 is shifted towards visible wavelength range due to N and Mn co-doping. Moreover, it is comparatively supported by the calculated band gap energies of all the catalysts using the formula $E_g = (1240/\lambda)$ [25]. The calculated band gap 3.18 eV of undoped TiO_2 is consistent with the value reported in the literature [26] whereas the co-doped samples values are ranging from 2.87 - 3.10 eV. Among the co-doped catalysts, NMn7 shows less band gap energy (2.87 eV), which has been diminished by 0.31 eV compared to undoped sample. The decreasing in band gap is may be ascribed to the mid-gap band states above valence band of TiO_2 formed by N 2p states. Thus the shift in absorbance from UV to visible region (red shift) caused due to decreased band gap can leads to generate more photo e^-/h^+ pairs, which favours better photocatalytic degradation efficiency in visible region [27].

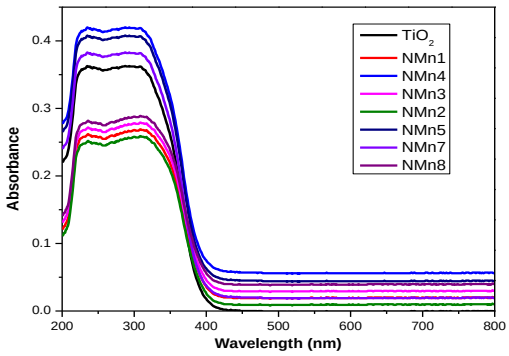

Fig. 2 UV-Vis. DRS spectra of undoped and N & Mn co-doped TiO_2 catalysts.

C. X-ray Photoelectron Spectroscopic (XPS) Analysis

Surface composition and oxidation states of N and Mn co-doped TiO_2 (NMn7) were investigated by XPS. Total survey spectrum and high resolution (HR) spectra of N, Mn, Ti and O are shown in Fig. 3. The existence of Ti^{+4} state was confirmed by the located binding energies of Ti $2p_{3/2}$ and Ti $2p_{1/2}$ components of NMn7 at 459.0 eV and 464.7 eV, respectively [28]. The deconvoluted peaks of Mn $2p_{3/2}$ and Mn $2p_{1/2}$ found at 644.13eV and 655.72 eV, respectively are correspond to Mn^{4+} suggesting that Mn^{4+} is substitutionally replaced Ti in TiO_2 [29]. The binding energy peak found at 399.6 eV is assigned to N 1S, which can be ascribed to the anionic N^- in O-Ti-N linkage [30-32]. This shift towards higher binding energy compared to TiN, that appears at ≤397.5 eV may be due to reduced electron density on the nitrogen caused by high electronegetivity of oxygen and it also evident by the observed shift in Ti $2p_{3/2}$ from 459.05 eV to 459.0 eV in undoped and NMn7 catalysts, respectively [33]. Further, it confirms that nitrogen incorporates and substitutes the oxygen in TiO_2 lattice. The O 1s peak fitted to two peaks at 530.1 eV and 532.3 eV, which are attributed to lattice oxygen in Ti-O bonds and oxygenated species like O^- and OH group that are weakly adsorbed on the surface [34].

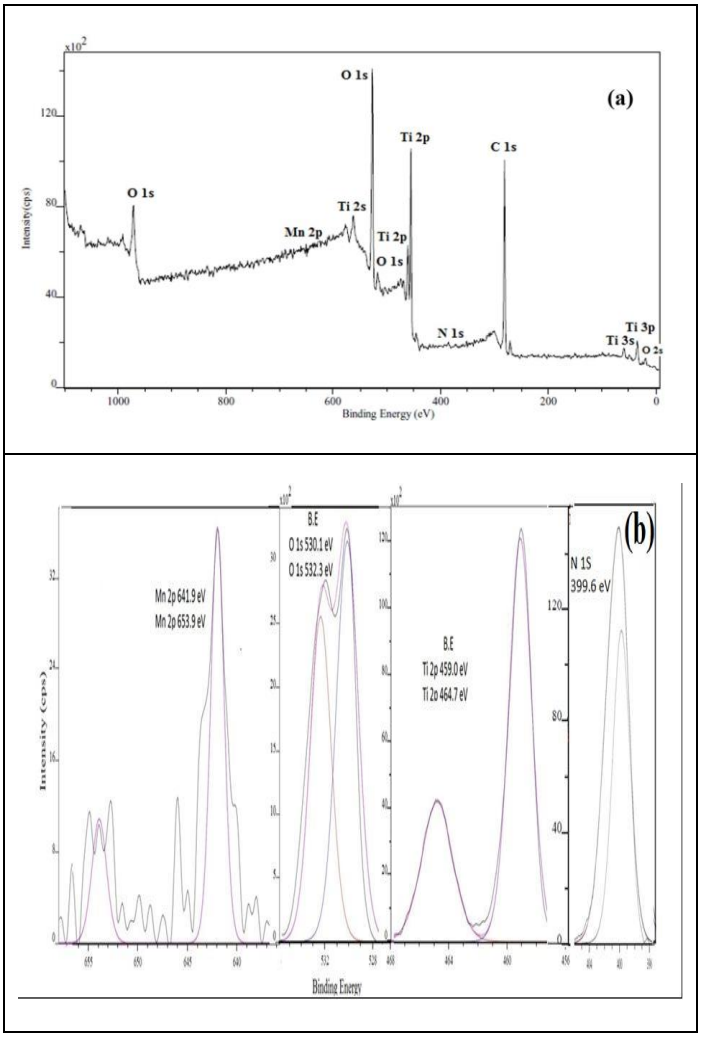

Fig. 3 (a) XPS survey spectrum of NMn7 (b) HR XPS spectra of Mn, O, Ti and N.

D. SEM and TEM Analysis

The microstructure analysis of the catalyst NMn7 was carried out by SEM and TEM analysis shown in Fig. 4 and 5(a-b). FESEM image shows small and spherical shaped particles distributed uniformly with less agglomeration whereas undoped TiO_2 [35] shows randomly shaped and aggregated particles.

TEM image (Fig.5(a)) showing spherical shaped nanoparticles with average particle size 9 nm. HRTEM image reveals that the NMn7 is completely crystalline, showing well defined lattice fringes with lattice spacing 3.51 A^0 of (101) planes of anatase TiO_2 [36]. Moreover, the TEM results are congruent to calculated crystallite size of NMn7 from its (101) peak in the XRD pattern. Finally, it confirms that, co-doping of N and Mn into TiO_2 lattice decreases the particle size of TiO_2, which leads to increased surface area and enhances its photocatalytic efficiency.

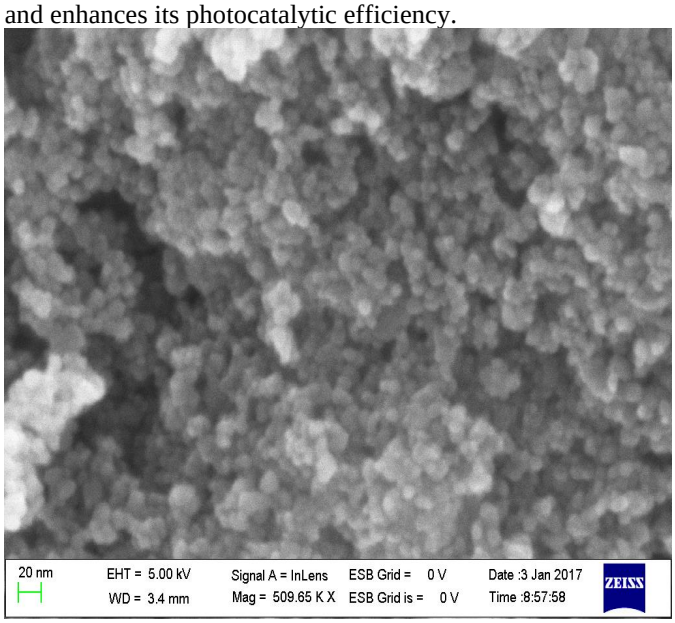

Fig. 4 FESEM image of co-doped TiO_2 (NMn7).

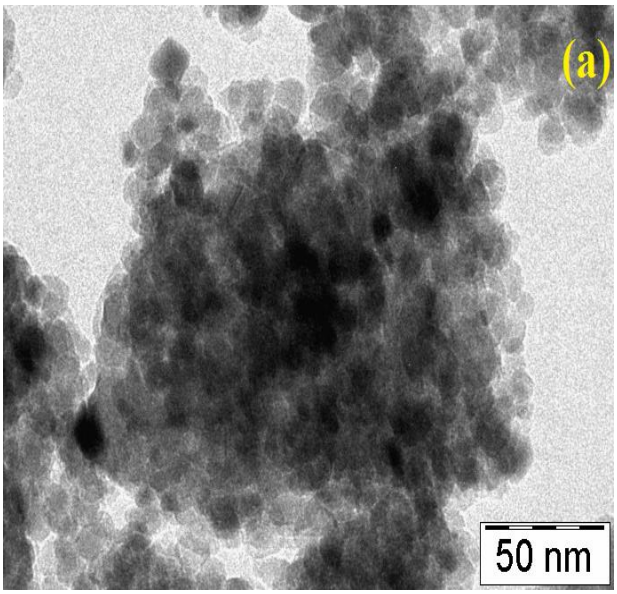

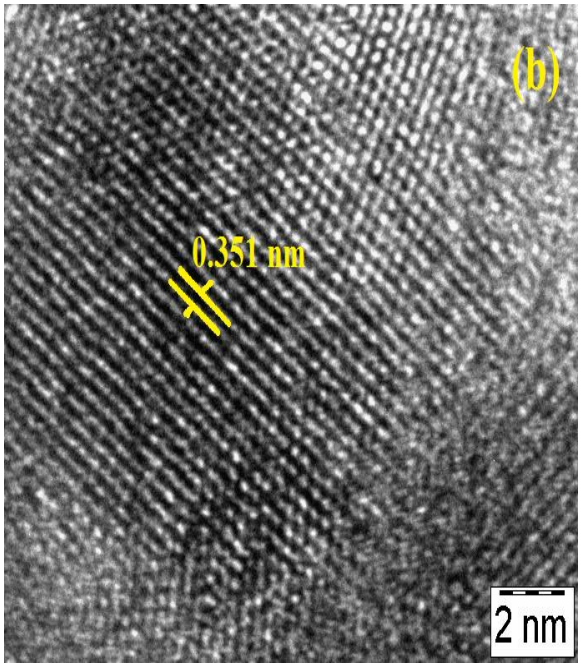

Fig.5 (a) TEM image of NMn7 (b) HRTEM image of NMn7

E. FT-IR Studies

FT-IR studies further confirmed the incorporation of dopants N and Mn into TiO_2 lattice. From Fig.6 peaks around 1620-1634 cm^{-1} and 3351-3450 cm^{-1} represents the bending and stretching vibrations of adsorbed H_2O and O-H, respectively. The Ti-O-Ti stretching frequency band at 513 cm^{-1} in undoped TiO_2 is shifted to 525 cm^{-1} in NMn7 catalyst showed that incorporation of dopants into TiO_2 lattice changed the Ti-O-Ti network and created the new interactions as Ti-N and Mn-O, which diminishes the octahedral coordination of Ti ions. The peaks at 1440 cm^{-1} and 601.1 cm^{-1} can be attributed to the Nitrogen and Manganese atoms substitute into TiO_2 network [37, 38]. Hence, substitutional doping of N and Mn into TiO_2 lattice by replacing O and Ti, respectively confirmed by FT-IR studies.

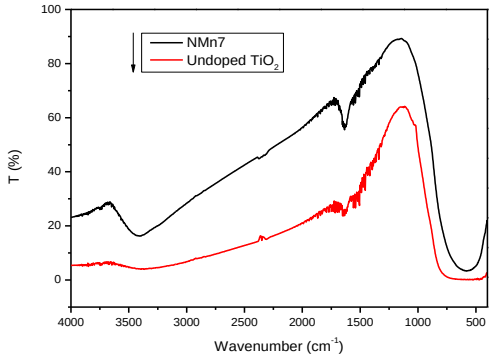

Fig. 6 FT-IR spectra of undoped TiO_2 and co-doped TiO_2 (NMn7)

F. Photo-Luminescent Spectral Studies

Photoluminiscence technique was performed by taking coumarin as a fluorescent probe to understand the production of $^{\bullet}OH$ responsible for oxidative degradation of pollutants in water during photocatalytic reaction [39].

In this technique coumarine solution (10 ppm) contains 0.1g of NMn7 in acidic conditions was irradiated under visible light. Upon the reaction with •OH coumarin forms the 7-hydroxy coumarin. To confirm this the PL intensity was measured from 250-600 nm with excitation wavelength fixed at 435 nm for the aliquots collected for every 30 min and represented in Fig. 7. It is noticed that in absence of irradiation (0 min) there was no absorption and while increasing irradiation time leads to increase in PL intensity confirms the enhanced rate of formation of •OH by the NMn7 is proportional to the irradiation time.

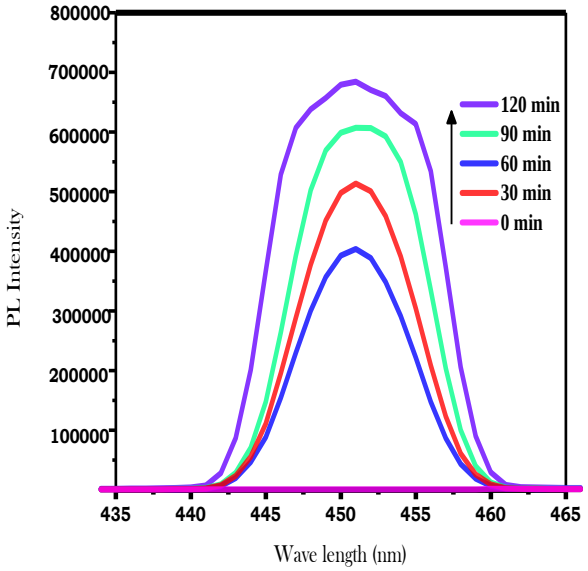

Fig. 7 Photoluminiscent spectra of NMn7 indicating the production of OH radicals when exposed to visible light.

IV. PHOTOCATALYTIC DEGRADATION AND OPTIMIZATION OF PARAMETERS

Photocatalytic degradation of malathion including blank test (without photocatalyst) was performed by following the procedure given in section 2.4. To attain the optimum reaction parameters for better photocatalytic degradation, the effect dopant concentration, pH, catalyst dosage, and initial pesticide concentration were studied one by one keeping other parameters constant.

A. Effect of dopant concentration

Malathion degradation studies using catalysts with various N and Mn dopant concentrations were carried out and results are shown in Fig. 8. Among all the nano catalysts, NMn7 showed best photocatalytic activity. The absorbance of malathion was gradually decreased with time and became almost zero after 250 min indicating complete degradation. This may be supported by decreased band gap, particle size and increased surface area in N (0.5 wt%) and Mn (1.00 wt%) co-doped TiO_2 (NMn7).

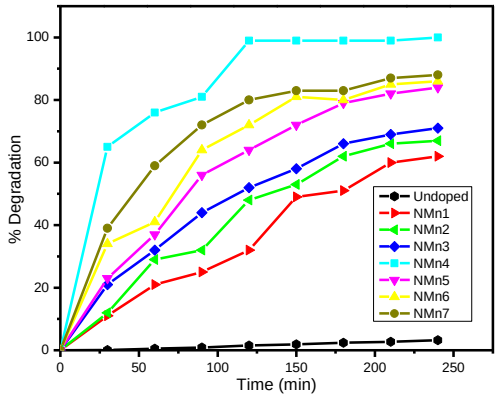

Fig. 8 Dopant concentration effect on % degradation of malathion by undoped and all N and Mn co-doped TiO_2 catalysts.

B. Effect of pH

The degradation of malathion was investigated under different pH conditions of 3, 8, 9 and 10 employing NMn7 as catalyst (which showed best catalytic performance) using 1.00 g/L catalyst and 10 mg/L dye solution. Based on the pH of the aqueous medium the surface of the TiO_2 obtains negatively or positively charged sites. From the experimental results presented in Fig.7, the photocatalytic degradation of malathion was faster at pH 9, because the point of zero charge value (pH-pzc) of TiO_2 is around 6.25 due to which it attains the negative charge and attracts more the malathion molecules [40] and similar findings were reported earlier [41].The better efficiency of degradation of malathion at higher pH values can be rationalised by the fact that the model pollutant will be in more beneficial to hydrolysis in alkaline solution than in acidic medium [42].

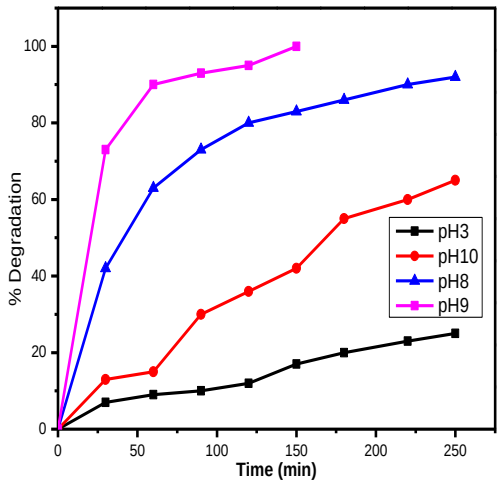

Fig. 9 Effect of pH on % degradation of malathion by NMn7.

C. Effect of catalyst dosage

To make sure the maximum absorption of visible light and reduce the catalyst wastage, an optimum catalyst dosage must be investigated.

Photocatalytic degradation studies carried out with different dosage (0.50- 2.00 g/L) of NMn7 at pH 9 and results are shown in Fig. 8. The optimum catalyst dosage was found to be 1.50 g/L and complete degradation was achieved in 150 min. The degradation rate was increased with increase in catalyst dosage up to 1.50 g/L. Generally augment in dosage of the catalyst facilitates the absorption of more number of photons, which generates much electrons and holes and thus enhances the production of hydroxyl radicals [•OH]. Also, the there will be an increase in adsorption of organic pollutants upon increasing catalyst dosage and facilitates the photocatalytic activity. However, turbidity and agglomeration of catalyst particles was observed if the catalyst dosage increased more than 1.50 g/L, due to which the light penetration is suspended and photocatalytic activity decreased [43]. The high catalyst dosage significantly effects the dispersion.

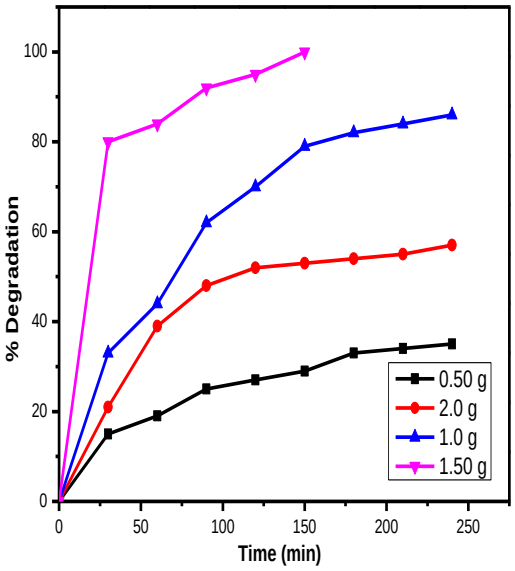

Fig. 10 Catalyst dosage effect on % degradation of malathion by NMn7.

D. Effect of initial pesticide concentration

The optimum initial pesticide concentration was attained by the experiments carried out by varying pesticide concentrations of 1, 5, 10 & 15 mg/L at fixed catalyst dosage and pH. From Fig.9 the optimum initial concentration of pesticide was found to be 5 ppm at pH 9 and catalyst dosage of 1.50 g/L. The rate of degradation is reduced if the concentration is more than 5 ppm because the fixed amount of catalyst cannot produce the sufficient •OH radicals to attack the increased number of pesticide molecules and also due to deactivation of the catalyst particles by blanket effect [44].

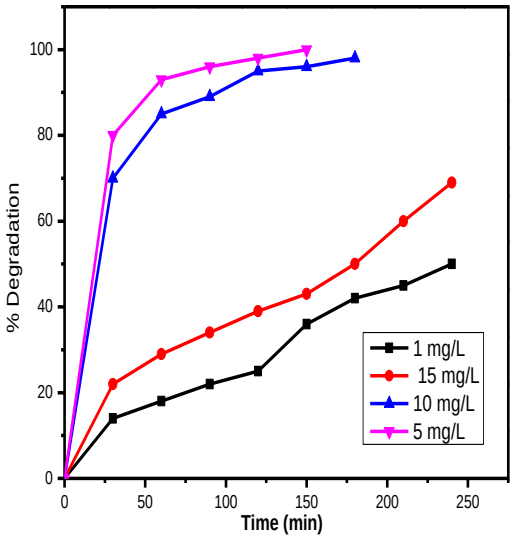

Fig. 11 Effect of initial malathion concentration on % degradation of malathion by NMn7.

V. POSSIBLE MECHANISM FOR PRODUCTION OF OH AND DEGRADATION OF MALATHION

Visible light + Catalyst → Catalyst ($h^+ + e^-$)

$h^+ + H_2O \rightarrow H^+ + {}^{\cdot}OH$

$h^+ + {}^{\cdot}OH \rightarrow {}^{\bullet}OH$

$e^- + O_2 \rightarrow {}^{\cdot}O_2^-$

$e^- + {}^{\cdot}O_2- + H_2O \rightarrow HO_2^{\cdot} + {}^{\cdot}OH$

$e^- + HO_2^{\cdot} + H^+ \rightarrow H_2O_2$

$e^- + H_2O_2 \rightarrow {}^{\bullet}OH + {}^{\cdot}OH$

•OH + Malathion→ Degradation Products

VI. CONCLUSION

Co-doping of Nitrogen and Manganese into TiO_2 matrix was successfully achieved by sol-gel method. The photocatalytic efficiency of synthesized catalyst was studied by degrading organophosphorous pesticide, malathion under visible light irradiation. The desired anatase phase with decreased band gap and particle size was achieved in all the synthesized nano catalysts. Nitrogen doping caused visible light response and Manganese doping improved the trapping of electrons and inhibiting e^-/h^+ recombination during photocatalytic process. Among all synthesized catalysts 0.50 wt% N & 1.00 wt% Mn-TiO_2 exhibited excellent in visible light photocatalytic activity. 100% degradation of malathion with initial concentration of 5 mg/L was achieved in 120 min at pH 9 with catalyst dosage of 1.50 g/L. It can be concluded that co-doping of TiO_2 with N and Mn is a promising route for enhanced photocatalytic degradation of pollutants in aqueous medium.

Retrieval Number: B3116129219/2019©BEIESP
DOI: 10.35940/ijeat.B3116.129219
Journal Website: www.ijeat.org

Published By:
Blue Eyes Intelligence Engineering
& Sciences Publication

ACKNOWLEDGMENT

Thota Susmitha is acknowledges to the University Grants Commission (UGC), New Delhi, India for project fellowship. Imandi Manga Raju is thankful to the DST-SERB for providing project fellowship.

REFERENCES

1. A.N. Kadam, R.S. Dhabbe, M.R. Kokate, Y.B. Gaikwad, K.M. Garadkar. Spectrochimica Acta Part A: Molecular and Biomolecular Spectroscopy. 133 (2014) 669–676.
2. N.A. Ramos-Delgado, M.A. Gracia-Pinill, L. Maya-Trevi˜no, L. Hinojosa-Reyes, J.L. Guzman-Mara, A. Hernández-Ramíreza. Journal of Hazardous Materials. 263 (2013) 36-44.
3. Imandi Manga Raju, T. Siva Rao, K.V. Divya Lakshmi, M. Ravi Chandra, J. Swathi Padmaja, G. Divya. Journal of Environmental Chemical Engineering 7 (2019) 103211.
4. Vincenzo Augugliaro, Claudio Baiocchi, Alessandra Bianco Prevot, Elisa García-López, Vittorio Loddo, Sixto Malato, Giuseppe Marcí, Leonardo Palmisano, Marco Pazzi, Edmondo Pramauro. Chemosphere 49 (2002) 1223-1230.
5. Jimmy C Yu, Lizhi Zhang, Zhi Zheng, Jincai Zhao. Chem Mater 15 (2003) 2280-2286.
6. Nick Serpone, Darren Lawless. Langmuir 10 (1994) 643-652.
7. M. Khairy, W. Zakaria. Egyptian Journal of Petroleum 23 (2014)419-426.
8. Kormann C, Bahnemann DW, Hofmann MR. Journal of Physical Chemistry 92 (1988)5196-5201.
9. Hariprasad N, Anju SG, Yesodharan EP, Yesodharan S. Research Journal of material science 1 (2013)9-17.
10. Hua Tang, Shufang Chang, Kongqiang Wu, Guogang Tang, Yanhui Fu, Qinqin Liu, Xiaofei Yang. RSC Advances 6 (2016) 63117-63130.
11. Meili Gu. RSC Advances, 5 (2015) 434–439.
12. J. Swathi Padmaja, T. Siva Rao, K.V. Divya Lakshmi, I. Manga Raju. Journal of Environmental Chemical Engineering 6 (2019) 6457-6467.
13. Sutassana Na Phattalung, Sukit Limpijumnong, JaejunYu. Applied Catalysis B: Environmental, 200 (2017) 1-9.
14. R.Jaiswal, J.Bharambe, N.Patel, Alpa Dashora, D.C.Kothari, A.Miotello. Applied Catalysis B: Environmental, 168–169 (2015) 333-341.
15. Roland Marschall, Lianzhou Wang. Catalysis Today 225 (2014)111-135.
16. Dvoranova D, Brezova V, Mazur M, Malathi MA. Applied Catalysis B: Environmental 37 (2002) 91-105.
17. Zhu J, Deng Z, Chen F, Zhang J, Chen H, Anpo M, Huang J, Zhang L. Appl Catal B: Environmental 62 (2006) 329-335.
18. Wu G, Nishikawa T, Ohtani B, Chen A. Chemistry of Materials 19 (2007)4530–4537.
19. Patil KR, Sathaye SD, Kollam YB, Deshpande SB, Pawaskar NR, Mandale AB. Materials Letters 57 (2003) 1775-1780.
20. Upkan UG, Hameed BH. Applied catalysis A: General 975 (2010)1-11.
21. Hongqi Sun, Yuan Bai, Wanqin Jin, Nanping Xu. Solar Energy Materials & Solar Cells 92 (2008) 76–83.
22. Lijie Wang, Xi Zhang, Peng Zhang, Zetan Cao, Junhua Hu. Journal of Saudi Chemical Society19 (2015) 595–601.
23. Dina MF, Mona BM. Journal of nanomaterials 524123 (2011) 1-8.
24. L. Gomathi Devi, Nagaraju Kottam, S. Girish Kumar. Journal of Physical Chemistry C 113 (2009) 15593–15601.
25. Hirotaka N, Koichi K, Masaahi T. Journal of Oleo Science 58 (2009) 389-394.
26. Karla R. Reyes-Gill, Enrique A. Reyes-Garcia, Daniel R. Journal of the electrochemical society 153 (2006) A1296-A1301.
27. Shaik Abdul Alim, T. Siva Rao, I. Manga Raju, M. Ravi Kumar, K.V. Divya Lakshmi. Journal of Saudi Chemical Society 23 (2019) 92–103.
28. Jimin Xiea, Deli Jianga, Min Chena, Di Li a, Jianjun Zhua, Xiaomeng Lüa, Changhao Yanb. Colloids and Surfaces A: Physicochem Engineering Aspects 372 (2010) 107–114.
29. Q.R. Deng, X.H. Xia, M.L. Guo, Y. Gao, G. Shao. Materials 65 (2011) 2051-2054.
30. M. Sathish, B. Viswanathan, R. P. Viswanath, Chinnakonda S. Gopinath. Chemistry of Materials 17 (25) (2005) 6349–6353.
31. Xiaobo Chen, Clemens Burda. Journal of Physical Chemistry B 108 (40) (2004) 15446–15449.
32. Hexing Li, Jingxia Li, Yuning Huo. Journal of Physical Chemistry B 110 (4) (2006) 1559–1565.
33. Ye Cong, Jinlong Zhang, Feng Chen, Masakazu Anpo. Journal of Physical Chemistry C 111 (2007) 6976-6982.
34. K.V. Divya Lakshmi, T. Siva Rao, J. Swathi Padmaja, I. Manga Raju, M. Ravi Kumar. Chinese Journal Chemical Engineering 27 (2019) 1630-1641.
35. Ravi Kumar Mulpuri, Siva Rao Tirukkovalluri, Manga Raju Imandi, Shaik Abdul Alim, Venkata Divya Lakshmi Kapuganti. Sustainable Environment Research 29 (2019) 29.
36. Ren Ren, Zhenhai Wen, Shumao Cui, Yang Hou, Xiaoru Guo, Junhong Chen. Scientific reports 5 (2015) 10714. DOI: 10.1038/srep10714.
37. Siriphan Chainarong, Lek Sikong, Sorapong Pavasupree, Sutham Niyomwas. Energy Procedia 9 (2011) 418-427.
38. Xiaojun_Ma, Wanru_Zhou, and Yin_Chen. Materials_(Basel) 10(6) (2017) 631.
39. Czili H, Horvath A. Applied Catalysis B: Environment 81 (2008) 295-302.
40. Selcuk H, Bekbolet M. Chemosphere 73 (2008) 854-858.
41. Fadaei AM, Dehghani M, Mahvi AH, Nasseri S, Rastkari N, Shayeghi M. E-Journal of Chemistry 9 (2012) 2015-2022.
42. Gangadhar B, Tharakeswar Y, Sujan Kumar K, Ramakrishna NG, Singhal RK. African Journal of Environmental Sciences and Technology 6 (2012) 224-228.
43. S. Liu, J.H. Yang, J.H. Choy Journal of Photochemistry and Photobiology A: Chemistry 179 (2006) 75–80.
44. N. Prabhakarrao, M. Ravi Chandra, T. Siva Rao. Journal of Alloys and Compounds 694 (2017) 596-606.

AUTHORS PROFILE

Dr. Sushmitha Thota, Department of Inorganic & Analytical Chemistry, School of Chemistry, Andhra University Visakhapatnam, India.

Dr. Gollamudi Padma Rao, Department of Chemistry, Dr. B.R. Ambedkar Univsity, Srikakulam, Andhrapradesh, India

Mr. Imandi Manga Raju, is pursuing his Ph.D at Andhra University, Visakhapatnam, India. His research of interest is synthesis and characterization of TiO_2 based nanomaterials for water pollution abatement. He published 8 research articles in reputed Scopus indexed peer reviewed Elsevier and Springer journals in the TiO_2 based nanomaterials.

Dr. T. Siva Rao, is a Professor at Dept. of Inorganic & Analytical Chemistry, Andhra University. He published 125 Research Articles in reputed peer reviewed international Journals. His areas of research interest are Heterogeneous Phtocatalysis, TiO_2 based nanomaterials. Organic – Inorganic nano hybrid materials.